A Novel Image Encryption with Deep Learning Model for Secure Content based Image Retrieval

Mohamed Elsharkawy[1,2], Ahmed N. Al Masri[3]

[1] BioImaging Lab, Department of Bioengineering, University of Louisville, Louisville, KY, USA

[2] Information Technology Department, Mansoura University, Mansoura, Egypt

[3]Department of Computer Science, American University in the Emirates, Dubai, United Arab Emirates

Emails: Mohamed.elsharkawy@louisville.edu ; ahmed.almasri@aue.ae

Abstract

From the last decades, a massive quantity of images gets generated and continues to rise to a maximum extent in the forthcoming data. The process of retrieving images based on a query image (QI) is a proficient method of accessing the visual properties from large datasets. Content-based image retrieval (CBIR) provides a way of effectively retrieving images from large databases. At the same time, image encryption techniques can be integrated into the CBIR model to retrieve the images securely. Therefore, this paper presents new image encryption with a deep learning-based secure CBIR model called IEDL-SCBIR. The proposed IEDL-SCBIR technique intends to encrypt the images as well as securely retrieve them. The proposed IEDL-SCBIR technique follows a two-stage process: optimal elliptic curve cryptography (ECC) based encryption and DL based image retrieval. The proposed model derives a cuckoo search optimization (CSO) with the ECC technique for the image encryption process in which the CSO algorithm is applied for optimal key generation. In addition, VGG based feature extraction with Euclidean distance-based similarity measurement is applied for the retrieval process. To validate the enhanced performance of the IEDL-SCBIR technique, a comprehensive results analysis takes place, and the obtained results demonstrate the betterment over the other methods.

Keywords: Content-based image retrieval; Security; Image encryption; Deep learning; Optimal key generation

1. Introduction

With the growth of imaging devices, like medicinal imaging equipment, digital cameras, and smartphones, people have faced a remarkable development in the importance, quantity, and availability of an image [1]. The need for effective image retrieval and storage service is strengthened by increasing largescale image datasets amongst each area. While, after the growth of the above two decades, the Content-Based Image Retrieval (CBIR) technique shows development to be helpful in various real-time image retrieval applications [2]. E.g., clinicians could utilize CBIR to find the related case of the patient and facilitate the medical for making decisions. But, a larger image dataset typically has millions of images. Occasionally, single digital images could be of twenty million dimensions, and their sizes can be over forty megabytes, namely mammography images [3]. Thus, the CBIR services generally incur computation complexities and higher storage. Cloud computing offers more significant opportunities for on-demand access to storage resources and sufficient computations, making it an exciting choice for CBIR outsourcing and image storage. With CBIR outsourcing service to the cloud servers, the data owners no longer needed to retain the image databases locally. The authorized image user could query the cloud servers for the CBIR services without communicating with the image owners. Despite the

DOI: https://doi.org/10.54216/JCIM.000105

remarkable benefit, image privacy has become the primary concern regarding CBIR outsourcing. E.g., the patient may not need to reveal their medicinal images to other people except certain physicians in medicinal CBIR application [4].

The CBIR technique retrieves and searches images from a dataset according to the feature extracted from an image. This work utilizes image class as beaches, Africa, buses, buildings, elephants, dinosaurs, food, flowers, mountains, and horses. The feature is extracted from the whole image database and saved in the feature vector [5]. Feature extraction with HSV histogram has color quantization, histogram computation, and color space transformation. Feature extraction with BSIF has patch selection from the gray image, the transformation of input RGB to gray images, patch whitening process, subtract mean value from each component, and evaluation of ICA elements [6]. CEDD feature extraction method has an HSV color two steps fuzzy connecting scheme. The color moment feature extraction method has the transformation of RGB to a single component and includes computation of standard deviation and mean of all the components. This saved feature vector is later related to the feature vector of query images [7]. The minimal distance with distance classifications like City block distance, Euclidean distance, Mahalanobis and Minkowski, leads to the retrieved comparisons. The detail of all the feature extraction processes is described in following sections. Compared with the present method with spatial and frequency domain features, in this work, two more BSIF and CEDD features to enhance the presented model's accuracy.

This paper presents new image encryption with a deep learning-based secure CBIR model called IEDL-SCBIR. The proposed IEDL-SCBIR technique intends to encrypt the images as well as securely retrieve them. The proposed IEDL-SCBIR technique follows a two-stage process: optimal elliptic curve cryptography (ECC) based encryption and DL based image retrieval. The proposed model derives a cuckoo search optimization (CSO) with the ECC technique for the image encryption process in which the CSO algorithm is applied for optimal key generation. In addition, VGG based feature extraction with Euclidean distance-based similarity measurement is applied for the retrieval process. To validate the enhanced performance of the IEDL-SCBIR technique, a comprehensive results analysis takes place, and the obtained results demonstrate the betterment over the other methods.

2. Literature Review

Xia et al. [8] proposed a system that supports CBIR on the encrypted image without disclosing the sensitive data to the cloud servers. First, the feature vector is extracted to represent the respective images. Next, the pre-filter table is made by the locality-sensitive hashing for increasing the search efficacy. Then, the feature vector is secure with the protected KNN model. Ferreira et al. [9] proposed a secured architecture for outsourcing privacy-preserving retrieval and storage in a huge image repository. This presented method depends upon the IES-CBIR model; a new Image Encryption System shows CBIR property. The result enables encrypted searching and storage with CBIR inquiries when maintaining privacy.

Xia et al. [10] presented a system that supports CBIR on encrypted images without disclosing sensitive data to the cloud servers. Initially, a feature vector is extracted for representing the respective image. Next, the pre-filter table is created with locality-sensitive hashing for increasing search efficacy. Furthermore, the feature vector is secure with the protected KNN model, and the image pixel is encrypted with typical stream ciphers. Additionally, consider the case that the legal query user might inappropriately distribute and copy the retrieved image to an unauthorized person, next proposed a watermark-based protocol to deter this unauthorized distribution.

Xia et al. [11] developed a privacy-preserving CBIR system that enables the data owners to outsource the image dataset and CBIR services to the cloud without disclosing the actual content of the databases to the cloud server. The local feature is employed to represent the image, and EMD is used to evaluate the resemblance of an image. The EMD computation is an LP problem. Nazir et al. [12] developed an innovative CBIR method for fusing features of texture and color. The CH is utilized for extracting color data. The texture feature is extracted with DWT and EDH. The feature is generated for every image and saved as feature vectors in the dataset. They calculated this study with work Corel 1-k datasets.

DOI: https://doi.org/10.54216/JCIM.000105

Liu et al. [13] proposed an efficient image retrieval model by integrating higher-level features from the CNN method and lower-level features from DDBTC. For example, the lower level features, color, and texture were created using vector quantization indexed histogram from DDBTC bitmap, maximal, and a minimal quantizer. On the other hand, higher-level features from CNN could efficiently take the person's point of view. By combining CNN and DDBTC features, the comprehensive DL 2 layer codebook features are made by the presented similarity reweighting, two layer codebooks, and reduction dimension for improving the entire retrieval rates.

Alzu'bi et al. [14] proposed a novel bilinear CNN-based framework with two similar CNN models as feature extractors. The activation of the convolution layer is utilized straightaway for extracting the image feature at different image scales and positions. The network framework is initiated with DCNN adequately pretrained on larger generic image datasets later finetuned for the CBIR tasks. Several distance measures present a hybrid feature-based effective CBIR scheme in Mistry et al. [15]. The spatial domain feature has color moments, color auto correlogram, frequency domain features, and HSV histogram features such as moment with SWT and feature with GWT method. Furthermore, to improve accuracy, binarized statistical image feature, edge, and color directivity descriptors feature is utilized to develop an effective CBIR scheme.

3. Design of IDEL-SCBIR Technique

In this study, a novel IEDL-SCBIR technique is derived from encrypting the images and securely retrieving them. The proposed IEDL-SCBIR technique follows a two-stage process: CSO-ECC-based image encryption process and VGG with Euclidean distance-based retrieval process. The detailed working of these processes is offered in the following sections.

3.1 Algorithmic Procedure of Optimal ECC Technique

The ECC is a public-key cryptographic approach that depends upon the algebraic framework of the elliptic curve on a finite field. It contains smaller keys above the non-EC cryptography (dependent upon plain Galois fields) to given comparable security. In ECC, the prime number is elected as n_p, and the private key is elected as H. Then, the ECC formulation is represented as:

$$E = p(i)^3 + u * p(i) + v \tag{1}$$

Where u and v are the constant values as $u = v = 2$. If the state $X = Y$ is achieved, an optimum point was elected to ECC. Afterward, X and Y are demonstrated in Eqs. (2) and (3).

$$X = mod(E, n_p) \tag{2}$$

$$Y = mod(p(j)^2, n_p) \tag{3}$$

Where $p(i,j)$ illustrates the points of the elliptic curve. n_p demonstrates the prime number. The doubling technique was employed to define X and Y measures [16]. An optimum point $P_e(k,l)$ and P_f is the public key where it can be signified as:

$$P_f = H * P_e \tag{4}$$

In this encryption procedure, every share has a block, and all the blocks are collected for encrypting. The number of blocks was represented as $b(i,j)$, where i and j are the row and column of the block. At this point, all the portions of data were given as an input for encrypted. Data $D_x(i,j)$ and $D_y(i+1,j)$, as well as the point, is demonstrated as:

$$C_1 = H * P_e \tag{5}$$

$$C_2 = (D_x, D_y) + C_1 \tag{6}$$

The private key (H) was employed to message decryption when decrypting the model, but point C_{11} was utilized for pixel point decryption.

$$C_{11} = H * C_1 \tag{7}$$

DOI: https://doi.org/10.54216/JCIM.000105

$$C_{ij} = C_2 - C_{11} \quad (8)$$

The C_{ij} stands for the ending result of the decrypted method. From the result of C_{ij}, pixels value of IR and original color bands (R, G, B) are saved uniquely. Eventually, the decrypting image is gained as:

$$F_{image} = R + G + B \quad (9)$$

The CSO technique optimally creates the keys employed in the encryption and decryption procedures. As with other evolutionary methods, the CSO begins with the primary population (population of cuckoos). This cuckoo has taken few eggs, which are placed in another species nests. Any eggs that look like the host eggs are further feasible that increase and turns into cuckoos. Other eggs have been noticed with the host and are demised. The rate of increased eggs depicts the suitability of the region. When further eggs exist in the region, it can be other profits to that region. Therefore, the condition that additional eggs have been survived is a parameter to the cuckoos that optimize.

The cuckoos search for an optimum region for maximizing their egg's life lengths. Then, they hatch and turn to mature cuckoos; society and the community can generate it. All the communities are their habitat to live. An optimum habitat of every community is the next target to cuckoo from other groups. Every group immigrates to an optimum present existing region. All groups are the resident from a region towards an optimum current existing region. An egg laying radius (ELR) has been computed concerning the number of eggs all the cuckoos place and their distance in the present optimizing region.

Then, the cuckoo begins laying eggs arbitrarily from the nests in its eggs, placing radii. This procedure remains still achieving the optimum location for egg placing (a zone with maximum profit). This optimizing zone has been putting in that the maximal amount of cuckoos collects together [17].

It can be essential for generating variables as an array that an optimized issue has been resolved. In GA and PSO, these arrays have been recognized by "chromosome" and "particles' positions"; however, in CSO, this array is named as "habitat".

In 1D $Nvar$ optimized issue, habitat is $1 \times Nvar$ array which depicts the present place of cuckoo life. It can be determined as:

$$Habitat = [x_1, x_2, \dots, x_{Nvar}] \quad (10)$$

The count of profit/suitability rate to the present habitat is reached as profit function estimation.

$$Porofit = f_p\,(habitat) = f_p(x_1, x_2, \dots, x_{Nvar}) \quad (11)$$

The COA has been a technique that maximizes profit functions. The cost function has been multiplied by a minus sign that the issue was resolved for utilizing CSO. For starting optimization, a habitat matrix-sized $N_{pop} \times N_{var}$ has been created. Then, the number of arbitrary eggs has been identified to all habitats matrix. All cuckoos lay 5- 20 eggs in nature. These numbers have been utilized as the maximal and minimal restrictions from the egg condition of all the cuckoos under distinct iterations. All the real cuckoos lay eggs from the particular range. Therefore, the maximal range of egg placing is the ELR. In an optimized issue, with the upper and lower limits of var_{hi} and var_{low}, all cuckoos have ELR that is equivalent to the entire amount of eggs, present amount of eggs, and the upper or lower limits of variables of the issue. Therefore, the ELR has been determined as:

$$ELR = \alpha \times \frac{Number\ of\ current\ cuckoos\ eggs}{Total\ number\ of\ eggs} \times (var_{hi} - var_{low}) \quad (12)$$

where α represents the variable that the maximal ELR is fixed. All the cuckoos arbitrarily place eggs from their host bird nest in their ELR. Afterward, each cuckoo putting its eggs, any eggs less like the host eggs have been recognized and thrown out. Therefore, in all eggs laying procedures, p% of every egg (generally 10%) whose profit function value has been lesser is destroyed.

The rest of the chicks from the host's nest are fed and higher. Another stimulating point on the cuckoo chicks is that only one egg is the opportunity that increased from all the nests. If the cuckoo chicks hatch, they can be throw out host eggs. When the host chicks hatch previous, the cuckoo chicks are

DOI: https://doi.org/10.54216/JCIM.000105

eaten the maximum food count (as their body is three times superior and it knocks another chick over). Then many days, the individual host chicks are die in hunger, and only the cuckoo chick is live. If the cuckoo chicks develop and become mature, they can survive from the neighboring location and its community to while. However, if the egg places time is close, it has immigrated for optimum habitats in that the chance to bring its eggs are superior. Then, the creating cuckoo groups from several locations (search space of the issue), the group with an optimum place has been chosen as the destination group to another cuckoo to immigrate.

Based on the detail that keeps the balance amongst the population of birds in nature, the number N_{max} has been utilized to control the maximal amount of cuckoos living from the location. This balance is because of competing for restricted food, being hunted with predators, and determining inappropriate nests to eggs.

3.2 Design of Image Retrieval Technique

The VGG-16 technique initially extracts the features during the image retrieval process, and then similarity measurement takes place. VGG network, the runner-up of the classification and localization track of the ILSVRC-2014 competitions, is considered a deep network framework using a smaller convolution filter of 3 × 3 than its predecessors, AlexNet. VGG-VD class presented 6 DCNN in the competitions; amongst them, two of them are very effective compared to other ones, such as VGG19and VGG16. The VGG16 has thirteen convolutional and three FC layers, whereas the VGG19 consists of sixteen and 3 FC layers. Both the networks use a stack of smaller convolution filters of 3 × 3 with stride one followed by many nonlinearity layers [18]. This increases the depth of the network and contributes to learning very complicated features. The impressive result of VGG exposed that the network depth is a significant factor in attaining higher classification performance. Fig. 1 demonstrates the framework of the VGG-16 model.

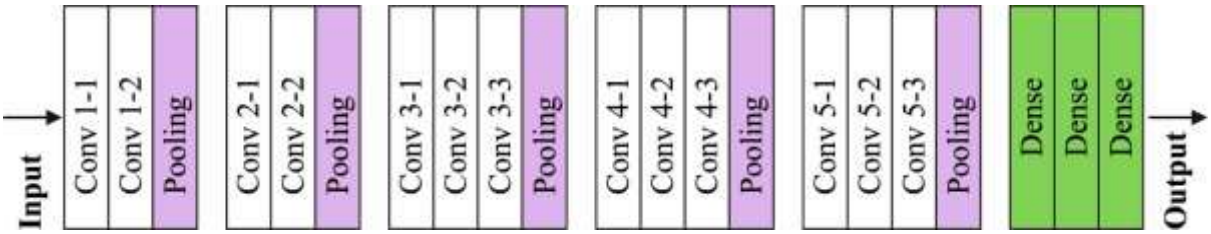

Fig. 1. VGG 16 Architecture

The feature vector of the QI and dataset images are represented by $F_eq = [F_eq(1), F_eq(2) \ldots\ldots F_eq(n)]$ and $F_eVdb = [F_eVdb(1), F_eVdb(2) \ldots\ldots F_eVdb(n)]$. The objective of the similarity matrices is to define the optimum 'n' relevant image from the databases similar to the QI. In this work, the Euclidean distance is utilized to the similarity measure denoted by Eq. (13).

$$E_d = \sqrt{\sum_{f=1}^{n} \left| \left(F_eV_{db}(f) - F_{e_q}(f) \right)^2 \right|} \tag{13}$$

Whereas n represents the feature vector length. F_eVq and F_eVdb represent the feature vector of the QI and dataset image correspondingly. While the distance becomes lower, the retrieval of images would be efficient.

4. Experimental Validation

The performance of the IEDL-SCBIR technique is simulated using Corel 10K dataset. The sample test images are illustrated in Fig. 2.

DOI: https://doi.org/10.54216/JCIM.000105

Fig. 2. Sample Test Image

The visualization results analysis of the IEDL-SCBIR technique is in Table 1 and Fig. 3, and the values pointed out the better performance of the IEDL-SCBIR technique with the higher PSNR. On the applied image 1, the IEDL-SCBIR technique has attained an increased PSNR of 47.595dB. Also, on the applied image 2, the IEDL-SCBIR method has gained a higher PSNR of 48.323dB. Moreover, on the applied image 3, the IEDL-SCBIR manner has attained a maximum PSNR of 46.409dB.

Table 1 Visualization of Encrypted and Decrypted Images of Proposed COA-ECC Model

Original Image	Encrypted Image	Decrypted Image	PSNR (dB)
	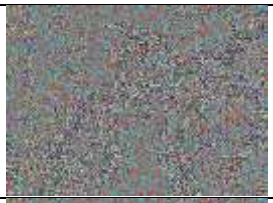		47.595
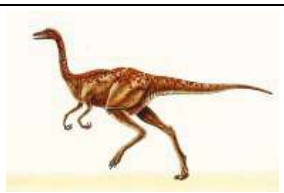		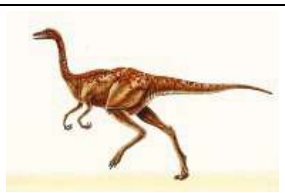	48.323
			46.409

DOI: https://doi.org/10.54216/JCIM.000105

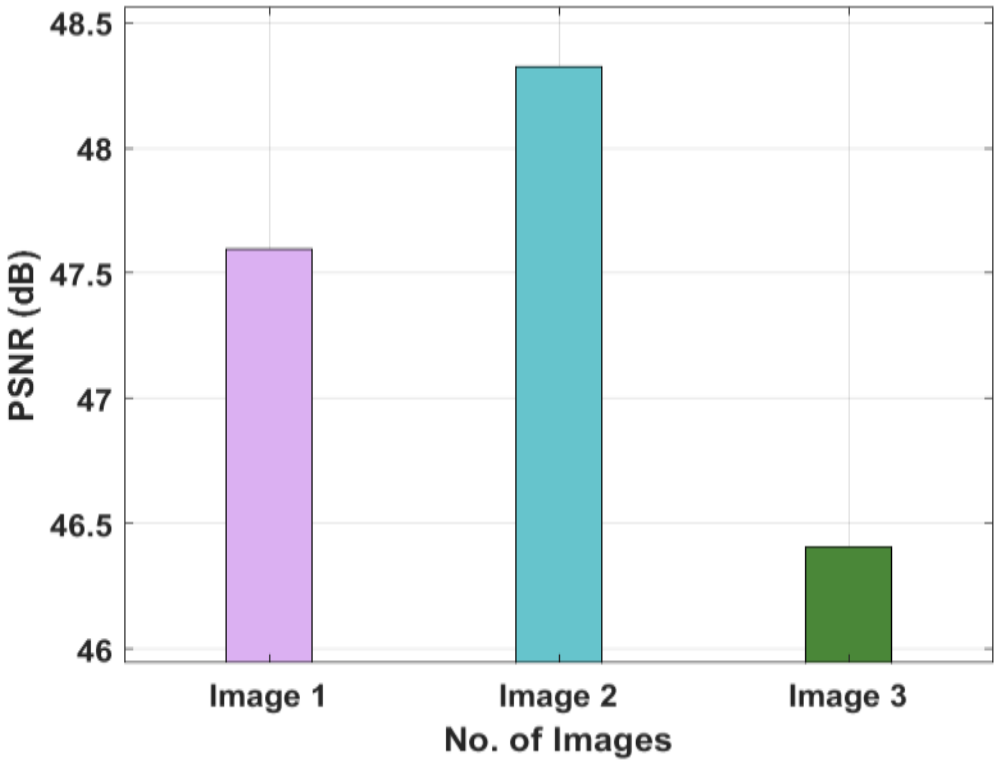

Fig. 3. PSNR analysis of IEDL-SCBIR model

A brief results analysis of the IEDL-SCBIR technique on the test images is given in Table 2 and Fig. 4. The figure portrayed that the IEDL-SCBIR technique can retrieve the images under distinct classes. It is reported that the IEDL-SCBIR technique has gained a higher average PRE_N and REC_N of 0.922 and 0.818.

Table 2 Results of Proposed Method in terms of Precision and Recall

No. of Class	Precision	Recall
Buses	0.967	0.867
Mountains	0.854	0.812
Beach	0.923	0.890
Elephants	0.845	0.789
Food	0.913	0.736
Flowers	0.983	0.813
Africa	0.890	0.883
Horses	0.971	0.848
Dinosaurs	0.978	0.790
Buildings	0.892	0.748
Average	0.922	0.818

DOI: https://doi.org/10.54216/JCIM.000105

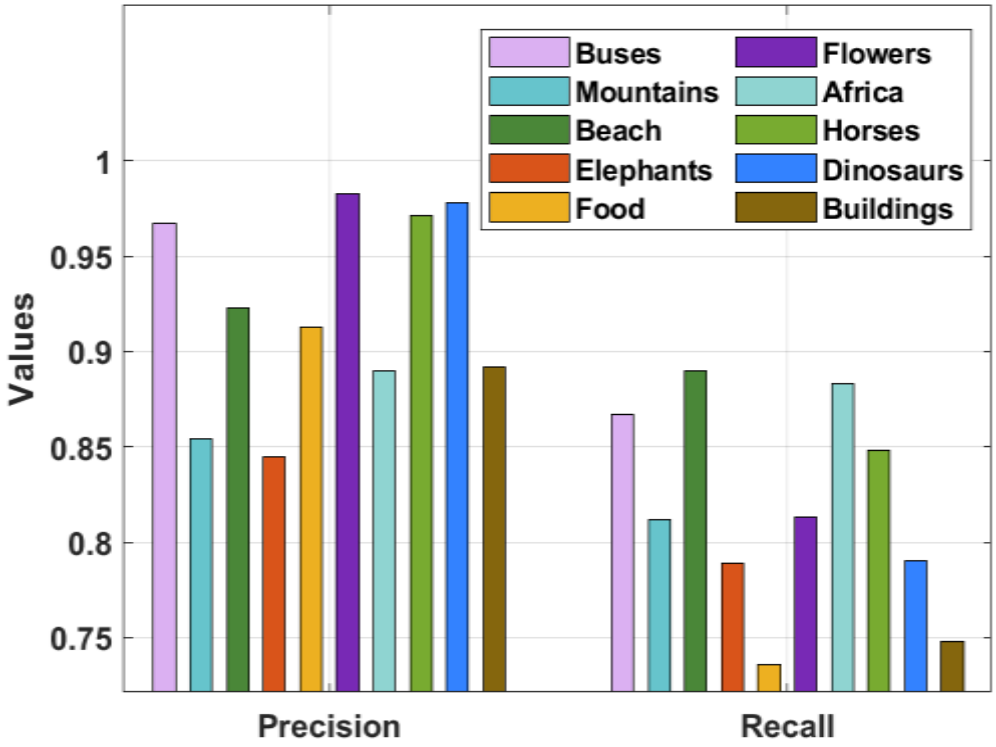

Fig. 4. Result analysis of IEDL-SCBIR model

A brief PRE_N analysis of the DL-VGG with existing techniques takes place in Table 3 and Fig. 5. The figure depicted that the DL-VGG technique has attained higher PRE_N on the test images. For instance, the DL-VGG technique has provided an increased PRE_N of 0.967, whereas the MA-CBIRS, IGA, and ENN techniques have attained a reduced PRE_N of 0.95, 0.84, and 0.95. The DL-VGG algorithm has provided an enhanced PRE_N of 0.983, whereas the MA-CBIRS, IGA, and ENN systems have reached a minimum PRE_N of 0.95, 0.97, and 0.95. Finally, the DL-VGG system has provided a superior PRE_N of 0.892, whereas the MA-CBIRS, IGA, and ENN manners have attained a decreased PRE_N of 0.74, 0.63, and 0.75.

Table 3 Comparison results of the proposed DL-VGG with other methods based on precision and average precision

No. of Class	DL-VGG	MA-CBIRS	IGA	ENN
Buses	0.967	0.95	0.84	0.95
Mountains	0.854	0.82	0.81	0.75
Beach	0.923	0.89	0.89	0.70
Elephants	0.845	0.82	0.72	0.80
Food	0.913	0.88	0.87	0.75
Flowers	0.983	0.95	0.97	0.95
Africa	0.890	0.83	0.82	0.65
Horses	0.971	0.95	0.95	0.90
Dinosaurs	0.978	0.99	0.82	1.00
Buildings	0.892	0.74	0.63	0.75
Average	0.922	0.88	0.83	0.82

DOI: https://doi.org/10.54216/JCIM.000105

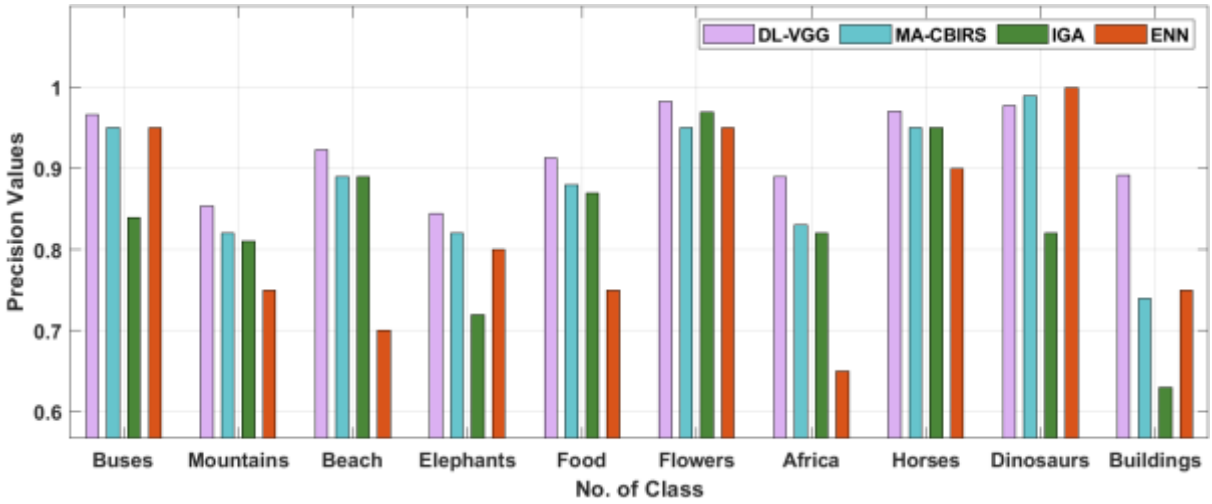

Fig. 5. Comparative analysis of DL-VGG model in terms of precision

Table 4 Comparison results of the proposed DL-VGG with other methods based on Recall and average Recall

No. of Class	DL-VGG	MA-CBIRS	IGA	ENN
Buses	0.867	0.74	0.73	0.19
Mountains	0.812	0.74	0.73	0.15
Beach	0.890	0.81	0.80	0.14
Elephants	0.789	0.55	0.53	0.16
Food	0.736	0.61	0.60	0.15
Flowers	0.813	0.65	0.64	0.19
Africa	0.883	0.71	0.70	0.13
Horses	0.848	0.85	0.84	0.18
Dinosaurs	0.790	0.74	0.72	0.20
Buildings	0.748	0.60	0.58	0.15
Average	0.818	0.70	0.69	0.16

A detailed REC_L analysis of the DL-VGG with recent approaches is in Table 4 and Fig. 6 [19]. The figure showcased that the DL-VGG technique has attained higher REC_L on the test images. For instance, the DL-VGG technique provides a maximum REC_L of 0.867, whereas the MA-CBIRS, IGA, and ENN systems have attained a reduced REC_L of 0.74, 0.73, and 0.19. At the same time, the DL-VGG technique has provided a superior REC_L of 0.813, whereas the MA-CBIRS, IGA, and ENN approaches have attained a minimum REC_L of 0.65, 0.64, and 0.19. Eventually, the DL-VGG method has provided an increased REC_L of 0.748, whereas the MA-CBIRS, IGA, and ENN methodologies have achieved a lower REC_L of 0.60, 0.58, and 0.15.

DOI: https://doi.org/10.54216/JCIM.000105

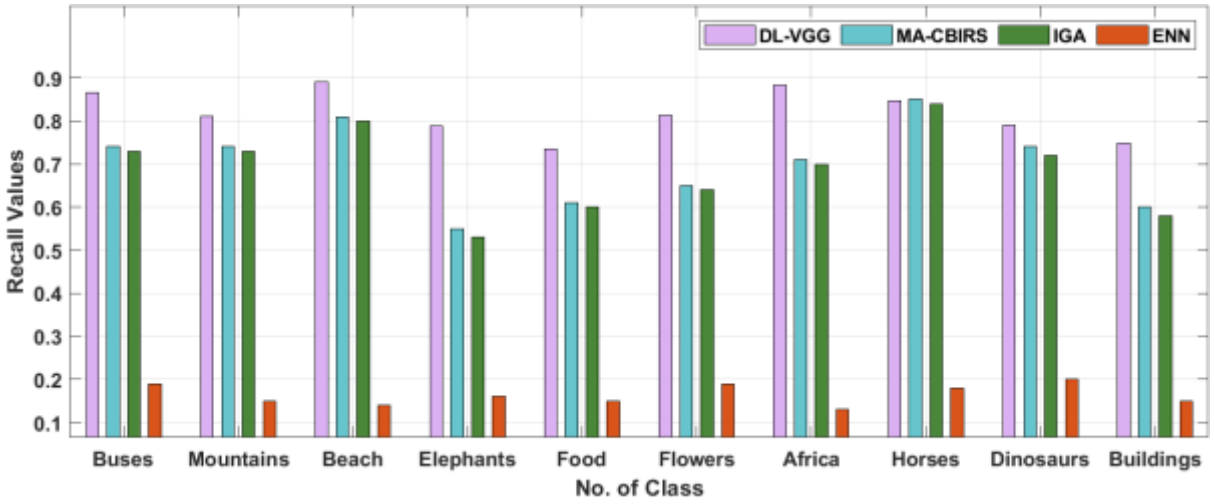

Fig. 6. Comparative analysis of DL-VGG model in terms of recall

5. Conclusion

In this study, a novel IEDL-SCBIR technique is derived from encrypting the images and securely retrieving them. The proposed IEDL-SCBIR technique follows a two-stage process: CSO-ECC-based image encryption process and VGG with Euclidean distance-based retrieval process. The proposed model derives a CSO with ECC technique for the image encryption process in which the CSO algorithm is applied for optimal key generation. In addition, VGG based feature extraction with Euclidean distance-based similarity measurement is applied for the retrieval process. To validate the enhanced performance of the IEDL-SCBIR technique, a comprehensive results analysis takes place, and the obtained results demonstrate the betterment over the other techniques. The experimental results stated the improvement of the IEDL-SCBIR technique and appeared as an effective tool for security and retrieval. As a part of the future scope, the IEDL-SCBIR technique can be extended to the cloud platform for secure data storage and transmission.

References

[1] Wan, J., Wang, D., Hoi, S.C.H., Wu, P., Zhu, J., Zhang, Y. and Li, J., 2014, November. Deep learning for content-based image retrieval: A comprehensive study. In Proceedings of the 22nd ACM international conference on Multimedia (pp. 157-166).

[2] Zhou, W., Li, H. and Tian, Q., 2017. Recent advance in content-based image retrieval: A literature survey. arXiv preprint arXiv:1706.06064.

[3] Tzelepi, M. and Tefas, A., 2018. Deep convolutional learning for content based image retrieval. Neurocomputing, 275, pp.2467-2478.

[4] Chung, Y.A. and Weng, W.H., 2017. Learning deep representations of medical images using siamese CNNs with application to content-based image retrieval. arXiv preprint arXiv:1711.08490.

[5] Piras, L. and Giacinto, G., 2017. Information fusion in content based image retrieval: A comprehensive overview. Information Fusion, 37, pp.50-60.

[6] Celik, C. and Bilge, H.S., 2017. Content based image retrieval with sparse representations and local feature descriptors: a comparative study. Pattern Recognition, 68, pp.1-13.

[7] Jin, C. and Ke, S.W., 2017. Content-based image retrieval based on shape similarity calculation. 3D Research, 8(3), pp.1-19.

[8] Xia, Z., Xiong, N.N., Vasilakos, A.V. and Sun, X., 2017. EPCBIR: An efficient and privacy-preserving content-based image retrieval scheme in cloud computing. Information Sciences, 387, pp.195-204.

[9] Ferreira, B., Rodrigues, J., Leitao, J. and Domingos, H., 2015, September. Privacy-preserving content-based image retrieval in the cloud. In 2015 IEEE 34th symposium on reliable distributed systems (SRDS) (pp. 11-20). IEEE.

[10] Xia, Z., Wang, X., Zhang, L., Qin, Z., Sun, X. and Ren, K., 2016. A privacy-preserving and copy-deterrence content-based image retrieval scheme in cloud computing. IEEE transactions on information forensics and security, 11(11), pp.2594-2608.

DOI: https://doi.org/10.54216/JCIM.000105

[11] Xia, Z., Zhu, Y., Sun, X., Qin, Z. and Ren, K., 2015. Towards privacy-preserving content-based image retrieval in cloud computing. IEEE Transactions on Cloud Computing, 6(1), pp.276-286.

[12] Nazir, A., Ashraf, R., Hamdani, T. and Ali, N., 2018, March. Content based image retrieval system by using HSV color histogram, discrete wavelet transform and edge histogram descriptor. In 2018 international conference on computing, mathematics and engineering technologies (iCoMET) (pp. 1-6). IEEE.

[13] Liu, P., Guo, J.M., Wu, C.Y. and Cai, D., 2017. Fusion of deep learning and compressed domain features for content-based image retrieval. IEEE Transactions on Image Processing, 26(12), pp.5706-5717.

[14] Alzu'bi, A., Amira, A. and Ramzan, N., 2017. Content-based image retrieval with compact deep convolutional features. Neurocomputing, 249, pp.95-105.

[15] Mistry, Y., Ingole, D.T. and Ingole, M.D., 2018. Content based image retrieval using hybrid features and various distance metric. Journal of Electrical Systems and Information Technology, 5(3), pp.874-888.

[16] Hemalatha, S., Rajamani, V. and Parthasarathy, V., 2017. Design of Optimal Elliptic Curve Cryptography by using Partial Parallel Shifting Multiplier with Parallel Complementary. International Journal of Computer Systems Science and Engineering, 32(5).

[17] Elyasigomari, V., Lee, D.A., Screen, H.R. and Shaheed, M.H., 2017. Development of a two-stage gene selection method that incorporates a novel hybrid approach using the cuckoo optimization algorithm and harmony search for cancer classification. Journal of biomedical informatics, 67, pp.11-20.

[18] Ha, I., Kim, H., Park, S. and Kim, H., 2018. Image retrieval using BIM and features from pretrained VGG network for indoor localization. Building and Environment, 140, pp.23-31.

[19] Alsmadi, M.K., 2018. Query-sensitive similarity measure for content-based image retrieval using meta-heuristic algorithm. Journal of King Saud University-Computer and Information Sciences, 30(3), pp.373-381.

DOI: https://doi.org/10.54216/JCIM.000105